

Linköping University Post Print

**The Role of Bowmans Layer in Corneal
Regeneration after Phototherapeutic
Keratectomy: A Prospective Study Using In
Vivo Confocal Microscopy**

Neil Lagali, Johan Germundsson and Per Fagerholm

N.B.: When citing this work, cite the original article.

Original Publication:

Neil Lagali, Johan Germundsson and Per Fagerholm, The Role of Bowmans Layer in Corneal Regeneration after Phototherapeutic Keratectomy: A Prospective Study Using In Vivo Confocal Microscopy, 2009, INVESTIGATIVE OPHTHALMOLOGY and VISUAL SCIENCE, (50), 9, 4192-4198.

<http://dx.doi.org/10.1167/iovs.09-3781>

Copyright: Research in Vision and Ophthalmology

<http://www.arvo.org/>

Postprint available at: Linköping University Electronic Press

<http://urn.kb.se/resolve?urn=urn:nbn:se:liu:diva-20753>

The role of Bowman's layer in anterior corneal regeneration after shallow-depth phototherapeutic keratectomy

A prospective, morphological study using in-vivo confocal microscopy

Neil Lagali, Johan Germundsson, and Per Fagerholm

Department of Ophthalmology, Linköping University Hospital
581 85 Linköping, Sweden

Supported by grants from the County Council of Östergötland (PF) and the Carmen and Bertil Regnérs Foundation (NL).

Disclosure: N. Lagali, None; J. Germundsson, None; P. Fagerholm, None.

Word count: 4121

Corresponding author and reprint request

Neil Lagali
Department of Ophthalmology
Linköping University Hospital
581 85 Linköping, Sweden
Tel +46 13 22 4658, Email: nlagali@ohri.ca

ABSTRACT

Purpose. To examine the role of Bowman's layer (BL) on the nature of anterior corneal regeneration after excimer laser phototherapeutic keratectomy (PTK) treatment.

Methods. A cohort of 13 patients received PTK to remove either 7 μ m of BL for treatment of primary recurrent corneal erosions (RCE; 6 patients) or complete BL removal (15 μ m ablation) to treat RCE or poor vision secondary to map-dot-fingerprint (MDF) dystrophy (7 patients).

Clinical examinations and laser-scanning in-vivo confocal microscopy (IVCM) were conducted preoperatively and at a mean of 4 and 8 months postoperatively.

Results. Total BL removal resulted in a significant decline in subbasal nerve density at 4 months ($P = 0.007$) which barely recovered to preoperative levels at 8 months ($P = 0.055$). With BL partially present, subbasal nerve density did not significantly change from preoperative levels. Superficial, wing, and basal epithelial cell density recovered to preoperative levels within 4 months after PTK regardless of the presence of BL. Subepithelial keratocytes, however, were more densely distributed in corneas without BL relative to those with a partial BL present ($P = 0.005$), and increased anterior keratocyte reflectivity was noted in all eyes without BL and in no eye with a partial BL present.

Conclusions. Subbasal nerve regeneration is delayed and subepithelial keratocyte density and reflectivity remain elevated up to 10 months after total BL removal by PTK. Our results provide initial evidence for a possible role of BL in facilitating rapid stromal wound healing and an associated recovery of anterior corneal transparency, and the restoration of epithelial innervation following epithelial trauma.

Key words: Bowman's layer, corneal regeneration, phototherapeutic keratectomy, recurrent corneal erosions, map-dot-fingerprint dystrophy, in-vivo confocal microscopy

Introduction

Bowman's layer (BL) is an acellular, non-regenerating layer located between the epithelial basement membrane and the anterior corneal stroma.¹ It is composed of randomly-oriented collagen fibrils within an extracellular matrix, is approximately 8 to 14 μ m thick in humans,² and is characterized by a smooth anterior surface facing the epithelial basement membrane and an indistinct posterior surface where it merges with the less dense, but ordered collagen lamellae of the corneal stroma proper.¹ Unmyelinated nerve axons penetrate BL irregularly across the cornea to ultimately provide epithelial innervation.³ While the precise functional role of BL remains to be elucidated, it has been suggested that BL may be superfluous to human corneal function considering the absence of adverse complications in hundreds of thousands of eyes that lack BL after having undergone excimer laser photorefractive keratectomy (PRK).⁴

In contrast, however, to its total removal in PRK, BL can be either removed or partially preserved in shallow-depth phototherapeutic keratectomy (PTK) treatment of anterior corneal disorders.⁵⁻¹⁷ PTK treatment of such disorders therefore provides a unique opportunity to assess the effect of the presence or absence of BL on corneal regeneration in response to anterior trauma. In addition to clinical measures of surgical outcome, a parallel morphologic investigation of PTK-treated corneas could yield insight into the role of BL in corneal recovery at the microscopic, sub-clinical level.

Accordingly, we undertook this study to prospectively follow two groups of patients (13 patients in total) indicated for unilateral, shallow-depth PTK. After the procedure, one group had approximately half the thickness of BL removed, while in the other group BL was removed fully. The treatment goal was to alleviate symptoms of recurrent corneal erosions (RCE) or to improve vision in patients with primary RCE or map-dot-fingerprint (MDF) dystrophy. We used laser-

scanning in-vivo confocal microscopy (IVCM) to obtain a detailed morphologic picture of cellular and nerve regeneration in the cornea after PTK treatment. IVCM is an ideal, non-invasive tool for examining the cornea at a morphologic, cellular level that is particularly well-suited for longitudinal observation,^{18,19} and corneal cell and nerve quantification.²⁰

Our primary aim in this study was to quantify anterior corneal morphology at the cellular level before and after PTK treatment using IVCM, to comparatively assess corneal regeneration with and without BL. Furthermore, it has been observed that although the use of PTK to treat anterior disorders of the cornea has been gaining popularity, there are surprisingly few prospective PTK studies²¹ and there is an absence of information concerning cellular and morphologic changes occurring during the postoperative healing phase. Accordingly, a secondary aim of this study was to provide a morphologic description of corneal regeneration after PTK.

Materials and Methods

Patients

A prospective cohort study was conducted with 13 eyes from 13 patients who received shallow-depth excimer laser PTK to treat recurrent corneal erosions (RCE) of various etiologies (12 patients, 6 with MDF dystrophy) or poor vision alone arising from MDF dystrophy (1 patient). The phototherapeutic keratectomies were consecutive cases performed by one of two surgeons (PF, JG) at the Linköping University Hospital from January to June 2008. Only eyes without prior surgical treatment were included in the study. All patients gave informed consent to participate, and the study followed ethical principles for research involving human subjects as stated in the tenets of the Declaration of Helsinki.

Preoperative evaluation

Patient charts were reviewed preoperatively to document symptoms and previous non-surgical treatments. All eyes with recurrent erosions had failed to respond to one or more conventional methods of treatment including topical medication with hyperosmotic agents or lubricants, therapeutic contact lenses or patching. Preoperative examination on the day of surgery included best-spectacle corrected visual acuity (BSCVA), slit-lamp photography and laser-scanning in-vivo confocal microscopy (IVCM; HRT3-RCM, Heidelberg Engineering, Heidelberg, Germany). A single operator (NL) performed all IVCM examinations; details of the IVCM procedure have been described elsewhere.²² For this study, IVCM was used to scan the corneal apical region to obtain a series of 400×400µm cross-sectional images through the full corneal thickness for subsequent nerve and cell quantification. In addition, the epithelium and anterior stroma was scanned laterally over several millimeters of central cornea to document any signs of pathologic morphology, with particular attention given to the epithelium, Bowman's layer, and the anterior stroma.

Surgical technique

Following application of local anaesthesia (tetracaine 1.0%, Novartis Ophthalmics, Täby, Sweden), corneal epithelium was removed mechanically with a #57 Beaver blade. All patients were then treated with a 193-nm ArF excimer laser system (Technolas 217, Bausch & Lomb) with a fluence of 120mJ/cm² and a repetition rate of 50Hz. The ablation depth was set to 15µm for complete removal of BL in MDF cases and 7µm for removal of half the thickness of BL in

other, non-dystrophic cases. The treatment zone was 7.0mm diameter of central cornea in all eyes.

Postoperative care and follow-up

Postoperatively, patients received Cincaïn® (cinchocaine hydrochloride 0.5%, Ipex Medical, Solna, Sweden) and Chloromycetin® (chloramphenicol 1%, Pfizer, Sollentuna, Sweden) eye ointments prior to installation of an eye patch. During the first postoperative day, Cincaïn® ointment was applied every four hours and one tablet of Dexofen® (Dextropropoxyphene 50mg, AstraZeneca, Södertälje, Sweden) was taken three times. Additionally, Chloromycetin® ointment was prescribed four times daily for the first five postoperative days. Follow-up examinations for this study occurred at 4 and 8 months postoperatively, and included assessment of symptoms, BSCVA, slit-lamp observation, and IVCN examination.

IVCM image analysis

From each IVCN examination, six en-face confocal images from the central cornea were selected by a single observer for quantitative analysis. The first image represented the corneal surface or superficial epithelium, which was the most anterior cell layer that could be visualized. The second image contained epithelial wing cells at a depth 20-25µm below the surface, the third image contained the most posterior epithelial cells or basal epithelium, and the fourth image contained nerve fiber bundles within the subbasal nerve plexus (subbasal nerves), located immediately posterior to the basal epithelium and running anterior to BL. The fifth and sixth images contained the most anterior layer of corneal keratocytes (without BL visible in the image), and stromal keratocytes 10-15µm posterior to the most anterior keratocyte layer,

respectively. These keratocytes, present within the anterior 5% of the corneal stroma, are hereafter referred to as ‘subepithelial keratocytes’ and were selected for analysis on the basis of their close apposition to the ablated region. BL itself was identified in IVCN images on the basis of its acellularity, slightly increased reflectivity relative to the anterior stromal extracellular matrix, and the visibility of nerve fiber bundles (in a Schwann cell sheath) comprising the underlying subepithelial nerve plexus.^{3,23} Acellularity was not used as the sole criteria for detecting BL, since cell-like structures resembling keratocyte nuclei were sometimes observed within BL in MDF patients. Cellular invasion of BL has been similarly noted in other corneal pathologies.⁴

A total of 234 images were selected for analysis (13 patients, 3 examinations/patient, and 6 images/examination). All images were randomized prior to analysis to mask observers to the patient, depth of ablation, and time of examination. Using ImageJ image processing software,²⁴ a 200×100µm (width×height) rectangle was superimposed onto each image of superficial, wing, and basal epithelial cells to highlight a region within the image containing cells with the most well-defined borders. For images of subepithelial keratocytes, a similar procedure was used, but with a 250×250µm square placed in the geometric center of the image. Within each selected region (rectangle or square), a bandpass filter was applied to attenuate high and low frequency noise (periodic variations below 2 pixels and above 80 pixels, respectively). In this manner, variations in background intensity were suppressed while cell or nuclear features were sharpened to maximize the ability of an observer to discriminate individual cells or nuclei (Figure 1).

Images with subbasal nerves were not pre-processed in any way prior to analysis.

Cells and nerves within 100% of the images were quantified by two independent observers (NL and JG) on separate occasions. Cells were counted manually by each observer with the assistance

of point-and-click cell marking and counting software.²⁴ Only cells with clearly distinguishable borders were counted. Cells crossing the top and right edges of the rectangular region were counted while those crossing the bottom and left edges were excluded. Additionally for stromal images, only in-focus bright objects presumed to represent keratocyte nuclei were counted. In cases of presumed fibroblast activity where multiple keratocyte nuclei appeared to aggregate into larger bright regions, an observer counted as many keratocyte nuclei as were presumed to exist within the region, based on region features and the size of surrounding distinct nuclei, similar to the method described by Patel et al.²⁵ Subbasal nerves were traced by a semi-automated method using nerve tracing software,²⁶ as described in detail elsewhere.²⁷ The total number of cells or total nerve length (in pixels) per image was recorded by both observers separately using commercial spreadsheet software (Excel 2003, Microsoft Corp, Redmond, WA, USA). Cell density (cells/mm²) or nerve density (µm/mm²) was calculated for each image, and images were unmasked to enable grouping according to cell type. Interobserver repeatability was determined by computing the 95% limits of agreement for each cell type using the method of Bland and Altman.²⁸ Prior to further statistical analysis, the mean cell or nerve density determined by the two observers was taken as the cell or nerve density for that image.²⁵ Additionally, the mean density of keratocyte nuclei from the two stromal images per cornea was taken to yield a single value of subepithelial keratocyte density per cornea.

From additional confocal scans obtained across a 3 to 4mm central region of each cornea, the presence of several morphologic features was determined: Bowman's layer (presence of at least two confocal images with BL characteristics posterior to the basal epithelium), a population of dendritic (Langerhans-type) cells at the level of the subbasal nerve plexus,²⁹ epithelial microcysts or 'dots',³⁰ characteristic irregularities and folds in the epithelial basement membrane ('map' or

‘fingerprint’ features),³⁰ and increased reflectivity of subepithelial keratocytes (relative to keratocyte reflectivity in deeper anterior stromal layers).

Statistical analysis

Cell and nerve density values were grouped according to time and PTK ablation depth. Time-dependent tests were performed on all study patients as a single group, and within two subgroups of patients (full and partial BL removal). For time-dependent comparisons, repeated measures analysis of variance (ANOVA) was used. One-way repeated measures ANOVA was used when normality and equal variance criteria for density values were met. Significant differences were isolated post-hoc using the Student-Newman-Keuls method. For normally-distributed data with unequal variances, we opted to use multiple paired t-tests over the non-parametric Friedman test due to the greater sensitivity of the paired t-test in the case of normally-distributed data.

Additionally, the two patient subgroups were compared at a fixed time using an independent t-test or the Mann-Whitney rank sum test. In all cases, the Kolmogorov-Smirnov procedure was used to test normality while equal variances were determined with the Levene median test. All statistical tests were two-tailed, and a P-value < 0.05 was considered statistically significant.

Statistical testing was performed with SigmaStat 3.5 statistical software (Systat Software Inc., Chicago, IL, USA).

Results

Clinical

The cohort consisted of 6 females and 7 males aged 48 ± 14 years (mean \pm SD) at the time of surgery. 12 patients had symptoms of recurrent corneal erosions, while one patient with MDF dystrophy was operated for poor vision. 54% of patients (7 eyes) had central corneal features consistent with MDF dystrophy, as determined by preoperative slit-lamp observation (Figure 2) and in-vivo confocal microscopy examination. The remaining 46% of patients (6 eyes) had recurrent corneal erosions of non-dystrophic origin (4 cases of corneal trauma and 2 idiopathic cases). All patients were examined preoperatively and at a mean of 4 (range 3-5) and 8 (range 6-10) months postoperatively. Preoperative and postoperative patient characteristics are given in Table 1. Phototherapeutic keratectomies were completed without intraoperative complications. At the final follow-up visit, mean BSCVA was 1.0 (20/20 Snellen equivalent, range 1.0 – 1.2), without reported recurrence of erosive events in any operated eye. The development of a persistent subepithelial haze during the postoperative period was a minor complication observed with the slit lamp in 3 MDF patients and in 1 RCE patient, with visual acuity appearing to be unaffected in all cases.

Cell quantification and analysis

The 95% limits of agreement for repeatability of interobserver cell and nerve density determination were superficial epithelium ($\pm 45\%$), epithelial wing cells ($\pm 14\%$), basal epithelium ($\pm 24\%$), subbasal nerves ($\pm 34\%$), and anterior stromal keratocytes ($\pm 31\%$).

Within the cohort, the density of subbasal nerves was significantly reduced ($P = 0.002$) at 4 months relative to the preoperative level. This reduction was followed by a significant increase from 4 to 8 months ($P = 0.009$) to establish a subbasal nerve density not significantly different ($P = 0.14$) from the preoperative level (Figure 3). Superficial, wing, and basal epithelial cell density and subepithelial keratocyte density after PTK did not significantly differ from preoperative levels (Table 2).

When sub-grouped by ablation depth, patients without BL exhibited recovery of epithelial cells and subepithelial keratocytes to preoperative density levels within 4 months. Subbasal nerve density, however, was significantly reduced at 4 months ($P = 0.009$) and remained reduced at 8 months relative to preoperative levels, although the reduction at 8 months failed to reach statistical significance ($P = 0.055$). By contrast, patients with a partial BL exhibited a less marked reduction in subbasal nerve density at 4 months followed by a more complete recovery at 8 months, without significant change from preoperative levels throughout the postoperative period. Additionally, epithelial wing cell density in patients with a partial BL increased significantly ($P = 0.03$) in the postoperative period.

Finally, comparison of patients with total BL removal to patients with a partial BL a fixed time yielded no significant differences in cell density before or after PTK, with the exception of subepithelial keratocytes, which had a significantly higher density after total BL removal compared with partial BL removal at 8 months ($P = 0.005$).

IVCM microstructural findings

Qualitative analysis of corneal morphology by IVCM revealed the presence of BL in all patients preoperatively. Postoperatively, BL was present in 6 of 6 patients who received PTK ablation to a depth of 7 μ m and in 0 of 7 patients who a 15 μ m ablation (Figure 4). A high density of dendritic cells was observed in the central cornea of 2 RCE and 2 MDF patients preoperatively. Of these patients, only one RCE patient did not exhibit dense dendritic cell population postoperatively. Additionally, in one RCE patient where dendritic cells were not observed preoperatively, a population of central dendritic cells was present postoperatively (Figure 5). Epithelial microcysts or ‘dots’ were present in 6 of 7 MDF eyes and in 3 of 7 RCE eyes preoperatively. At the latest follow-up, no dots were found in any eye. Central corneal map regions were observed in all MDF eyes preoperatively, while only one eye had observable fingerprint lines. Postoperatively, no fingerprint lines were found while map regions persisted in two MDF eyes (Figure 6). At the latest follow-up, subepithelial keratocytes exhibited increased reflectivity in 7 of 7 patients without BL and in 0 of 6 patients with a partial BL (Figure 6).

Discussion

Our PTK treatment strategy of complete BL removal in MDF patients and partial preservation of BL otherwise was clinically successful. No recurrence of symptoms was reported and all patients had excellent vision up to 10 months postoperatively. Subbasal nerves – which were completely removed during surgery – only partially regenerated after 4 months while substantial recovery occurred after 8 months. A delay in nerve regeneration was observed in patients without BL relative to patients with a partial BL. In cases of total BL removal, the subepithelial nerve fiber

bundles directly posterior to BL (comprising the subepithelial nerve plexus, which subsequently penetrate BL to give rise to the nerves of the subbasal nerve plexus)^{3,31} may have been damaged or completely removed along with the removal of BL. No nerves from the subepithelial nerve plexus were observed in IVCM images after total BL removal, although the increased anterior stromal reflectivity in these corneas may have masked their presence. By contrast, in eyes with a partial BL present, nerves of the subepithelial plexus were observed posterior to BL in IVCM images. From these observations, it appears that in the absence of both BL and the underlying subepithelial plexus, subbasal nerves are slow to recover as they would presumably regenerate from peripheral nerves outside the treatment zone or from deeper stromal nerves. On the other hand, with a partial BL present, preservation of the underlying subepithelial nerve plexus would promote faster regeneration of central subbasal nerves. It is postulated that in cases of epithelial trauma BL may therefore serve a role as a protective barrier to the underlying subepithelial nerve plexus – the presence of which provides for quick recovery of the subbasal nerves essential for epithelial innervation and restoration of the protective corneal aversion reflex.³²

In our cohort, the density of cells within the various epithelial layers recovered to preoperative levels within the first few postoperative months. Apart from map regions present within the treatment zone in two MDF patients, the regenerated epithelium after PTK appeared morphologically normal under confocal microscopic examination. Moreover at any given time, epithelial, nerve and subepithelial keratocyte densities were apparently independent of the presence of BL, with the only exception being a significant increase in subepithelial keratocyte density 8 months postoperatively in corneas without BL. This increased density manifested in the confocal images as an aggregation of keratocytes into regions of increased scatter, interpreted as

wound healing fibroblast activity.^{33,34} Trauma from the deeper ablation (reaching the anterior stromal surface) likely resulted in prolonged stromal activation and wound healing.

Qualitatively, by IVCN we observed a persistent stromal activation in all cases where BL was removed and an absence of activation where BL was present. Clinically, a mild subepithelial haze was present upon slit lamp examination. A similar mild or transient postoperative haze has been reported in some patients after shallow-depth PTK,^{11,13,35} and our morphologic findings suggest that this haze may be more prevalent at the subclinical, morphologic level, particularly in patients without BL. Similar morphologic findings by IVCN have been reported in the context of PRK, where subsequent normalization of keratocyte density and reflectivity was associated with restoration of corneal transparency and disappearance of haze at a minimum of 12 months after the procedure.³³ It has been suggested that only wounds that traverse BL into the stroma result in prolonged myofibroblast transformation.³⁴ Our present observations of subepithelial keratocyte activity therefore suggest a further possible function of BL in accelerating the process of anterior stromal wound healing and the restoration of corneal transparency after epithelial trauma.

It is interesting to note that the possible functions of BL outlined above are consistent with observations of a sensory deficit and postoperative haze in PRK-treated eyes devoid of BL.^{33,34,36} Although an ‘apparent lack of significant complications’ has been suggested in the hundreds of thousands of PRK-treated eyes devoid of BL,⁴ we suggest that future epithelial trauma in these eyes may result in prolonged stromal wound healing and recovery of transparency and corneal sensation, as compared to eyes with BL present.

The clinical outcome in our cohort suggests a re-examination of shallow-depth treatment strategy in MDF patients presenting with recurrent erosions. Non-zero rates of recurrence have been reported in MDF patients who received PTK ablation to a depth of 5 to 8 μm ^{7,8,10,14,16,35} and in RCE patients (with and without dystrophy) who received ablation as shallow as 5 μm .^{13,37} On the other hand, in 15 MDF patients who received PTK ablation to a mean depth of 10 μm , Pogorelov and co-workers reported no recurrence of erosion after a mean follow-up of 4.8 years¹¹ while Örndahl and Fagerholm reported one instance of recurrence in ten patients who received PTK ablation to a mean depth of 11 μm , after a mean follow-up period of 24 months.¹² For MDF patients both in this prospective study and in an earlier series of 10 MDF patients treated in our clinic for recurrent erosions with a mean ablation depth of 16 μm , no recurrences were reported, with a mean follow-up time of 25 months (range 13 – 47 months) in the earlier series.³⁸ These studies indicate a possible association between post-PTK recurrence in MDF patients and the partial presence of BL. Improved outcome following repeat procedures of 5 to 7 μm -depth PTK^{8,14,16,37} (which would result in total BL removal) provides support for such an association. We surmise that in some cases of MDF where BL may be affected, partial ablation of BL may not be sufficient to prevent recurrence of the underlying pathology.

We noted in this study that in patients with clinical symptoms of RCE, reliance on slit lamp findings alone can sometimes make accurate differential diagnosis of idiopathic RCE from MDF dystrophy difficult. In a retrospective study of 22 patients with MDF dystrophy, Labbé and co-workers reported 3 patients (13.6%) with a normal corneal structure on slit lamp examination who were diagnosed with MDF dystrophy only after IVCM examination.³⁰ In our cohort, one presumed RCE patient was similarly re-diagnosed with MDF dystrophy after map, dot, and

fingerprint features were observed with IVCN. The preoperative examination in this case enabled us to modify the PTK treatment strategy for complete BL removal. In this patient, a preoperative visual acuity of 0.4 (20/50 Snellen equivalent) subsequently improved to 1.0 (20/20) after six months without recurrence of erosion. We suggest that IVCN may be a useful screening tool for presumed RCE patients prior to PTK treatment. Additionally, IVCN may also be useful in determining preoperative BL thickness prior to PTK. Given the inter-individual variability in BL thickness,³⁹ it is conceivable that in some patients total BL removal may not be achieved with an ablation depth of 15 μ m, and conversely in some patients with a thin BL, 7 μ m ablation may result in total BL removal.

Dendritic cells were observed in a few patients in this study, both before and after PTK, and exhibited a morphology consistent with both mature (cells bearing dendritic processes) and immature forms (cell bodies only).^{29,40} High densities of dendritic cells residing in the central cornea are thought to accompany irritation,⁴¹ wound healing,²⁹ or inflammation,^{29,40,41} all of which may have been present to varying degrees in the corneas examined in this study. The significance of our findings of dendritic cells is unclear. Given the ongoing discussion surrounding the interpretation of findings of dendritic cells in the central cornea,⁴⁰ a more detailed study of their relationship to RCE, MDF dystrophy, and the PTK treatment is warranted.

One limitation of this study was the small size of the central corneal region used for quantitative analysis. Because many MDF patients did not have map, dot, or fingerprint features present at the central apical region, the cell density values (for wing and basal epithelial cells) would not represent the 'true' density averaged over a larger corneal region. The true density would be

lower due to an apparent acellularity in regions with microcysts or basement membrane folds. Accordingly, although epithelial cell densities as reported in this study did not generally change after PTK treatment, an absence of map, dot, or fingerprint features after treatment would have likely resulted in a marked increase in epithelial cell density, if a larger corneal area were to be considered.

A relatively high interobserver variability was reported in the quantification of a few of the corneal parameters in this study. Borders of superficial epithelial cells were often difficult to detect due to a high specular reflection, variable reflectivity and desquamation of epithelial cells,²² and a general reduction in image contrast of this outermost corneal layer as visualized with the laser-scanning in-vivo confocal microscope. Additionally, basal epithelial cell borders were sometimes indistinct, and subepithelial keratocytes were sometimes difficult to quantify in the presence of high background reflectivity (in the wound healing phase). The best agreement was for epithelial wing cells due to their dark cytoplasm with highly reflective cell borders. Considering our analysis of 100% of images by both observers and given the nature of the corneas, the limits of interobserver agreement are reasonable in comparison to other studies employing a similar method of analysis.^{42,43}

In conclusion, while the absence of BL does not appear to impede recovery of stratified epithelial morphology following shallow-depth PTK, two potential roles of BL following epithelial trauma in the human cornea have been identified. BL may present a physical barrier to protect the subepithelial nerve plexus and thereby hasten epithelial innervation and sensory recovery, and may also serve as a barrier to prevent direct traumatic contact with the corneal stroma to

accelerate stromal wound healing and the associated restoration of anterior corneal transparency at the morphologic level. Further studies with a larger patient population could provide additional evidence to support these putative roles.

References

1. Kenyon, KR. Morphology and pathologic responses of the cornea to disease. In: Smolin G and Thoft RA (eds.) *The Cornea. Scientific foundations and clinical practice*. Boston: Little, Brown and Co.; 1983:45.
2. Hogan MJ, Alvarado JA, Weddell. *Histology of the human eye*. Philadelphia: W.B. Saunders Company; 1971:82.
3. Klyce SD, Beuerman RW. Structure and function of the cornea. In: Kaufman HE et al. (eds.) *The Cornea*. New York: Churchill Livingstone; 1988:3-54.
4. Wilson SE, Hong J-W. Bowman's layer structure and function. Critical or dispensable to corneal function? A hypothesis. *Cornea* 2000;19:417-420.
5. Fagerholm P. Phototherapeutic keratectomy: 12 years of experience. *Acta Ophthalmol Scand* 2003;81:19-32.
6. Förster W, Atzler U, Ratkay I, Busse H. Therapeutic use of the 193-nm excimer laser in corneal pathologies. *Grafe's Arch Clin Exp Ophthalmol* 1997;235:296-305.
7. Chow AMM, Yiu EPF, Hui MK, Ho CK. Shallow ablations in phototherapeutic keratectomy: long-term follow-up. *J Cataract Refract Surg* 2005;31:2133-2136.

8. Jain S, Austin DJ. Phototherapeutic keratectomy for treatment of recurrent corneal erosion. *J Cataract Refract Surg* 1999;25:1610-1614.
9. Lohmann CP, Sachs H, Marshall J, Gabel VP. Excimer laser phototherapeutic keratectomy for recurrent erosions: a clinical study. *Ophthalmic Surg Lasers* 1996;27:768-772.
10. Dinh R, Rapuno CJ, Cohen EJ, Laibson PR. Recurrence of corneal dystrophy after excimer laser phototherapeutic keratectomy. *Ophthalmology* 1999;106:1490-1497.
11. Pogorelov P, Langenbucher A, Kruse F, Seitz B. Long-term results of phototherapeutic keratectomy for corneal map-dot-fingerprint dystrophy (Cogan-Guerry). *Cornea* 2006;25:774-777.
12. Örndahl MJF, Fagerholm PP. Phototherapeutic keratectomy for map-dot-fingerprint corneal dystrophy. *Cornea* 1998;17:595-599.
13. Baryla J, Pan YI, Hodge WG. Long-term efficacy of phototherapeutic keratectomy on recurrent corneal erosion syndrome. *Cornea* 2006;25:1150-1152.
14. Bernauer W, De Cock R, Dart JKG. Phototherapeutic keratectomy in recurrent corneal erosions refractory to other forms of treatment. *Eye* 1996;10:561-564.

15. Maini R, Loughnan MS. Phototherapeutic keratectomy re-treatment for recurrent corneal erosion syndrome. *Br J Ophthalmol* 2002;86:270-272.
16. Stewart OG, Pararajasegaram P, Cazabon J, Morrell AJ. Visual and symptomatic outcome of excimer phototherapeutic keratectomy for corneal dystrophies. *Eye* 2002;16:126-131.
17. Cavanaugh TB, Lind DM, Cutarelli PE, Mack RJS, Durrie DS, Hassanein KM, Graham CE. Phototherapeutic keratectomy for recurrent erosion syndrome in anterior basement membrane dystrophy. *Ophthalmology* 1999;106:971-976.
18. Calvillo MP, McLaren JW, Hodge DO, Bourne WM. Corneal reinnervation after LASIK: prospective 3-year longitudinal study. *Invest Ophthalmol Vis Sci* 2004;45:3991-3996.
19. Darwish T, Brahma A, Efron N, O'Donnell C. Subbasal nerve regeneration after penetrating keratoplasty. *Cornea* 2007;26:935-940.
20. Patel DV, McGhee CNJ. Contemporary in vivo confocal microscopy of the living human cornea using white light and laser scanning techniques: a major review. *Clin Exp Ophthalmol* 2007;35:71-88.
21. Öhman L, Fagerholm P. The influence of excimer laser ablation on recurrent corneal erosions: a prospective randomized study. *Cornea* 1998;17:349-352.

22. Eckard A, Stave J, Guthoff RF. In vivo investigations of the corneal epithelium with the confocal rostock laser scanning microscope (RLSM). *Cornea* 2006;25:127-131.
23. Guthoff RF, Baudoin C, Stave J. *Atlas of confocal laser scanning in-vivo microscopy in ophthalmology*. Berlin: Springer Verlag; 2006.
24. Abramoff MD, Magelhaes PJ, Ram SJ. Image processing with ImageJ. *Biophotonics Int* 2004;11:36-42.
25. Patel SV, McLaren JW, Hodge DO, Bourne WM. Normal human keratocyte density and corneal thickness measurement by using confocal microscopy in vivo. *Invest Ophthalmol Vis Sci* 2001;42:333-339.
26. Meijering E, Jacob M, Sarria JCF, Steiner P, Hirling H, Unser M. Design and validation of a tool for neurite tracing and analysis in fluorescence microscopy images. *Cytometry* 2004;58:167-176.
27. Lagali NS, Griffith M, Shinozaki N, Fagerholm P, Munger R. Innervation of tissue-engineered corneal implants in a porcine model: a 1-year in vivo confocal microscopy study. *Invest Ophthalmol Vis Sci* 2007;48:3537-3544.
28. Bland JM, Altman DG. Statistical methods for assessing agreement between two methods of clinical measurement. *Lancet* 1986;1:307-310.

29. Mastropasqua L, Nubile M, Lanzini M, Carpineto P, Ciancaglini M, Pannellini T, Di Nicola M, Dua HS. Epithelial dendritic cell distribution in normal and inflamed human cornea: in vivo confocal microscopy study. *Am J Ophthalmol* 2006;142:736-744.
30. Labbé A, De Nicola R, Dupas B, Auclin F, Baudouin C. Epithelial basement membrane dystrophy: evaluation with the HRT II Rostock Cornea Module. *Ophthalmology* 2006;113:1301-1308.
31. Guthoff RF, Wienss H, Hahnel C, Wree A. Epithelial innervation of the human cornea: a three-dimensional study using confocal laser scanning fluorescence microscopy. *Cornea* 2005;24:608-613.
32. Müller LJ, Marfurt CF, Kruse F, Tervo TMT. Corneal nerves: structure, contents and function. *Exp Eye Res* 2003;76:521-542.
33. Møller-Pedersen T, Cavanagh HD, Petroll M, Jester JV. Stromal wound healing explains refractive instability and haze development after photorefractive keratectomy: a 1-year confocal microscopic study. *Ophthalmology* 2000;107:1235-1245.
34. Tervo T, Moilanen J. In vivo confocal microscopy for evaluation of wound healing following corneal refractive surgery. *Prog Ret Eye Res* 2003;22:339-358.

35. Sridhar MS, Rapuno CJ, Cosar B, Cohen EJ, Laibson PR. Phototherapeutic keratectomy versus diamond burr polishing of Bowman's layer in the treatment of recurrent corneal erosions associated with anterior basement membrane dystrophy. *Ophthalmology* 2002;109:674-679.
36. Erie JC, McLaren JW, Hodge DO, Bourne WM. Recovery of subbasal nerve density after PRK and LASIK. *Am J Ophthalmol* 2005;140:1059-1064.
37. O'Brart DPS, Muir MGK, Marshall J. Phototherapeutic keratectomy for recurrent corneal erosions. *Eye* 1994;8:378-383.
38. Germundsson JR, Fagerholm PP. Treatment of map-dot-fingerprint corneal dystrophy with phototherapeutic keratectomy. (manuscript in preparation).
39. Li HF, Petroll WM, Møller-Pedersen T, Maurer JK, Cavanagh HD, Jester JV. Epithelial and corneal thickness measurements by in vivo confocal microscopy through focusing (CMTF). *Curr Eye Res* 1997;16:214-221.
40. Zhivov A, Stachs O, Kraak R, Stave J, Guthoff RF. In vivo confocal microscopy of the ocular surface. *Ocular Surf* 2006;4:81-93.

41. Zhivov A, Stave J, Vollmar B, Guthoff R. In vivo confocal microscopic evaluation of langerhans cell density and distribution in the corneal epithelium of healthy volunteers and contact lens wearers. *Cornea* 2007;26:47-54.

42. McLaren JW, Patel SV, Nau CB, Bourne WM. Automated assessment of keratocyte density in clinical confocal microscopy of the corneal stroma. *J Microscopy* 2008;229:21-31.

43. Niederer RL, Perumal D, Sherwin T, McGhee CNJ. Corneal innervation and cellular changes after corneal transplantation: an in vivo confocal microscopy study. *Invest Ophthalmol Vis Sci* 2007;48:621-626.

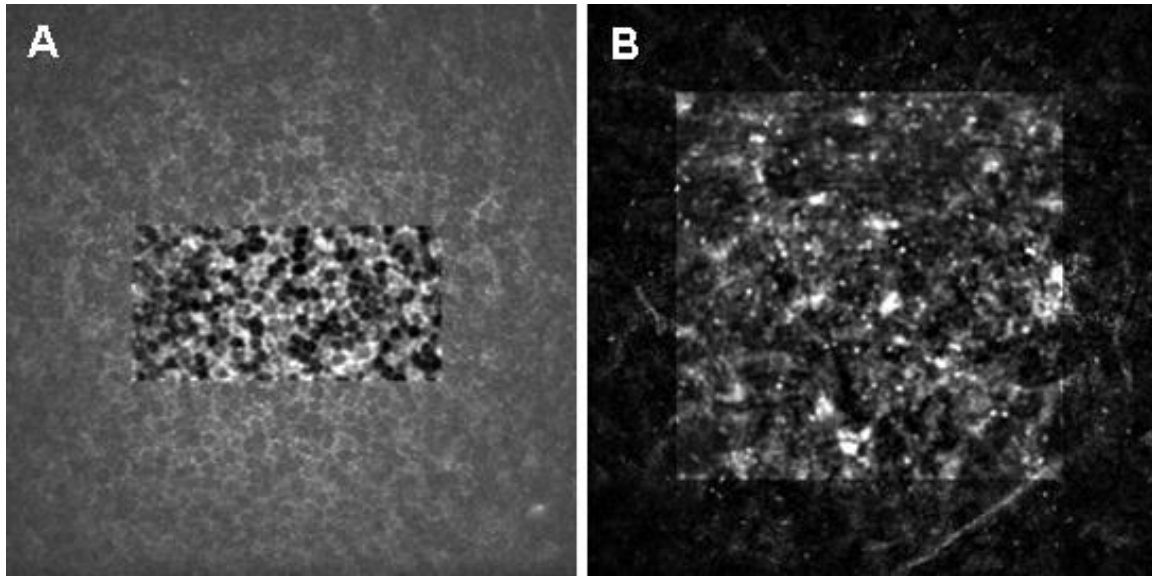


Figure 1. The appearance of pre-processed IVCM images prior to cell counting. Bandpass filtering within the region of interest enhanced the ability to visualize borders of distinct cells. (A) $200 \times 100 \mu\text{m}$ region of interest in the basal epithelial cell layer. (B) $250 \times 250 \mu\text{m}$ region of interest in the subepithelial stroma.

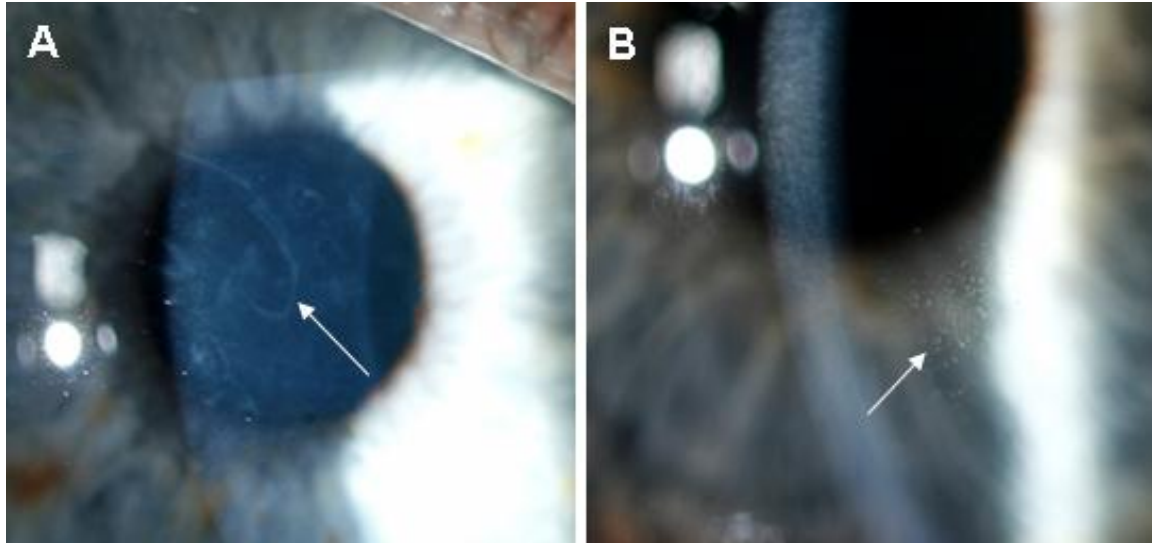


Figure 2. Preoperative slit lamp photographs of corneas from (A) a 57-year-old male patient with map-dot-fingerprint dystrophy, with geographic map regions clearly visible (arrow), and (B) a 33-year-old female with recurrent corneal erosions, with dot-like epithelial deposits (arrow).

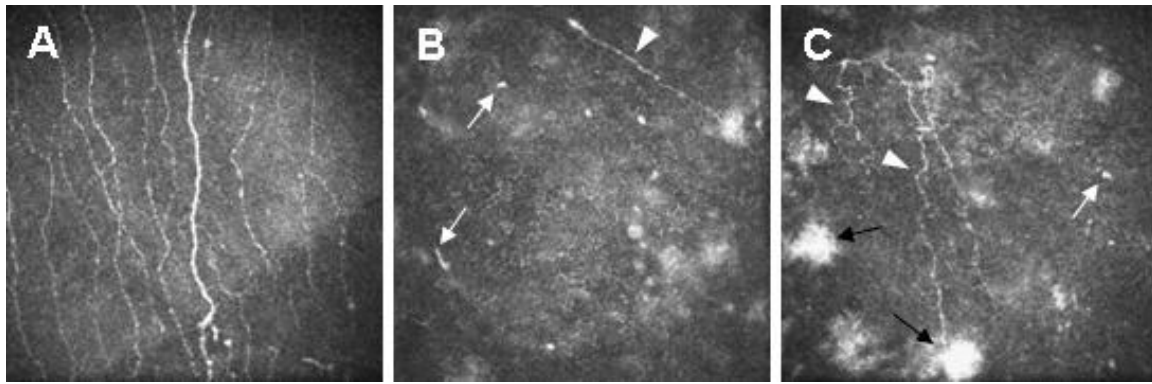


Figure 3. Subbasal nerve regeneration after PTK in a 29-year-old female with MDF dystrophy. (A) Preoperative subbasal nerve plexus. (B) 4 months after PTK, presumed sprouting subbasal nerves (white arrows) and a regenerating subbasal nerve (arrowhead) present at the basal epithelium. (C) 7 months after PTK, presumed sprouts (white arrow) and mildly tortuous regenerated subbasal nerves (arrowheads) are visible at the basal epithelium. Activity in the subepithelial keratocyte layer is observed in the same image frame (black arrows) indicating the absence of BL. Image size 400×400μm.

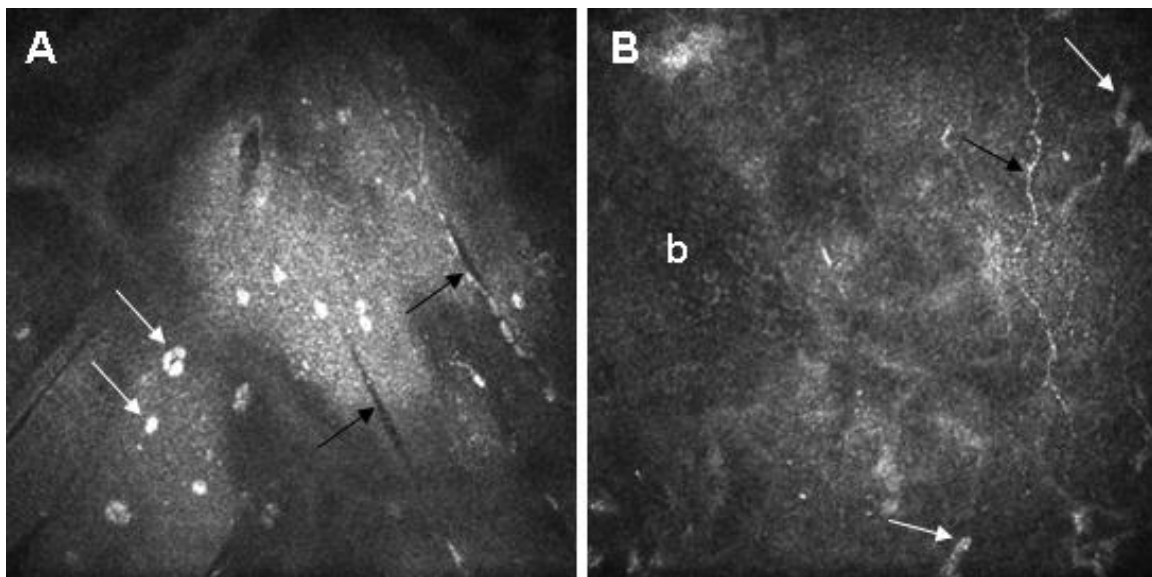


Figure 4. Corneal morphology in a 31-year-old female with MDF dystrophy. (A) Pre-PTK, BL exhibits increased reflectivity in patches, with narrow folds evident (black arrows) and unidentified cell or nuclear inclusions present within BL (white arrows). (B) 7 months after PTK, basal epithelial cells (b), keratocyte nuclei (white arrows), and a regenerated subbasal nerve (black arrow) are present at the same corneal depth, indicating the absence of BL. Image size 400×400μm, depth of images from corneal surface (A) 43μm, (B) 46μm.

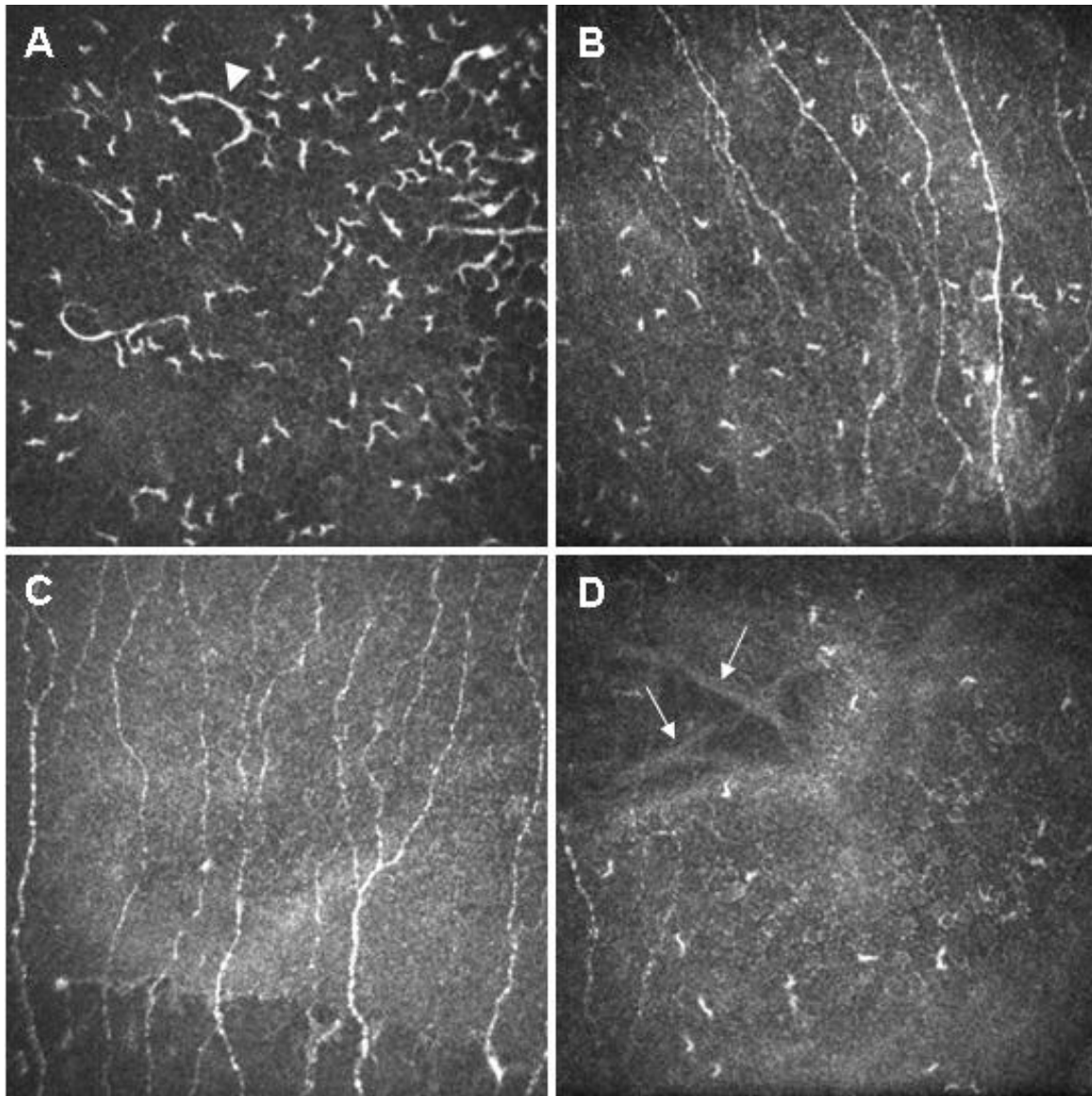


Figure 5. Basal epithelial layer in the central cornea of a 33-year-old female RCE patient (A,B) and in a 39-year-old female RCE patient (C,D). (A) Preoperatively, dendritic cell bodies, some with dendrites (arrowhead) occupied the central cornea (>100 cells per field). (B) 9 months postoperatively, a population of dendritic cell bodies remains (>50 per field). (C) Preoperatively, the basal epithelium is free of dendritic cell bodies. (D) 8 months postoperatively, dendritic cell bodies are present (25 per field). Note the presence of a partial BL with posterior surface defined by the existence of subepithelial nerve fiber bundles (arrows). Image size 400×400μm, depth of images from corneal surface (A) 40μm, (B) 42μm, (C) 52μm (D) 52μm.

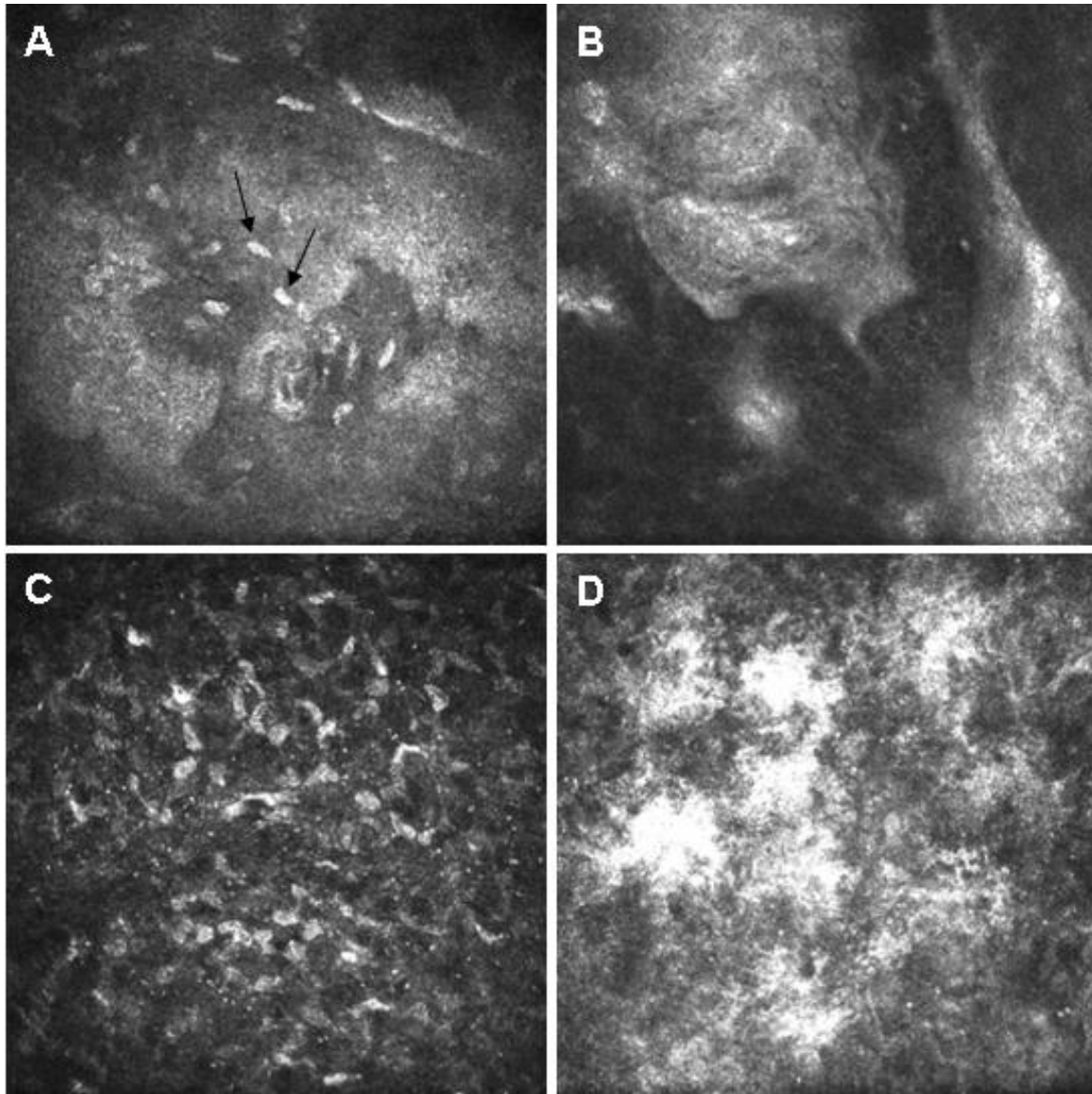


Figure 6. Geographic map regions in the central cornea of a 65-year-old male MDF patient (A,B) and the most anterior stromal layer in the central cornea of a 50-year-old male MDF patient (C,D). (A) Preoperative map region with presumed activated keratocytes present (black arrows). (B) 4 months postoperatively, a map region is present at the level of the basal epithelium. (C) Preoperatively, distinct keratocyte nuclei were visible just posterior to BL. (D) 7 months postoperatively, patches of increased stromal reflectivity were observed just posterior to the basal epithelium. Image size $400 \times 400 \mu\text{m}$, depth of images from corneal surface (A) $69 \mu\text{m}$, (B) $45 \mu\text{m}$, (C) $52 \mu\text{m}$ (D) $39 \mu\text{m}$.

Patient No.	Age	Gender	Condition	Eye	Ablation depth (μm)	BSCVA		Final follow-up (months)	Postoperative Complications*
						Preop	Final		
1	33	F	RCE	OS	7	1.0	1.2	9	subepithelial haze
2	39	F	RCE	OD	7	1.0	1.0	8	
3	30	M	RCE	OD	7	1.0	1.0	7	
4	63	M	RCE	OS	7	0.9	1.0	8	
5	52	M	RCE	OD	7	1.0	1.0	9	
6	50	F	RCE	OD	7	0.5	1.0	8	
7	29	F	MDF	OS	15	1.0	1.0	7	subepithelial haze
8	60	F	MDF	OS	15	0.2	1.0	10	
9	57	M	MDF	OS	15	1.0	1.0	6	
10	65	M	MDF	OD	15	0.7	1.0	7	
11	50	M	MDF	OS	15	1.0	1.0	7	
12	31	F	MDF	OD	15	0.4	1.0	6	subepithelial haze
13	65	M	MDF	OD	15	1.0	1.0	6	subepithelial haze

Table 1. Clinical characteristics of the study cohort.

* ‘subepithelial haze’ indicates a diffuse hazy appearance or discrete, punctate, or fleck opacities

PTK ablation depth	Cell layer	Time of examination			ANOVA p-value*
		Preoperative	4m	8m	
All (N = 13)	A	1163 \pm 272	1115 \pm 268	1113 \pm 311	0.90
	B	5729 \pm 1018	6219 \pm 799	6063 \pm 654	0.21
	C	9538 \pm 995	9273 \pm 1480	9517 \pm 1756	0.84
	D	15669 \pm 9483	5447 \pm 3541	10553 \pm 6467	0.002/0.009/0.14
	E	735 \pm 249	815 \pm 240	725 \pm 229	0.54
15 μm (N = 7)	A	1243 \pm 306	1118 \pm 251	1189 \pm 353	0.79
	B	6000 \pm 851	5893 \pm 381	5757 \pm 642	0.69
	C	9717 \pm 1223	9125 \pm 564	9207 \pm 1808	0.57
	D	16180 \pm 10660 \ddagger	3918 \pm 2411 \ddagger	9280 \pm 4897	0.009\ddagger
	E	852 \pm 245	801 \pm 190	858 \pm 188	0.88
7 μm (N = 6)	A	1071 \pm 215	1113 \pm 311	1025 \pm 256	0.88
	B	5413 \pm 1181 \ddagger \S	6600 \pm 1017 \ddagger	6421 \pm 498 \S	0.03
	C	9329 \pm 694	9446 \pm 2192	9879 \pm 1784	0.80
	D	15072 \pm 8870	7231 \pm 4004	12038 \pm 8166	0.07/0.13/0.63
	E	630 \pm 223	733 \pm 169	535 \pm 128	0.22

Table 2. Mean (\pm SD) cell or nerve density in the cohort. Cell layers are defined as follows. A: superficial epithelial cells (cells/mm²), B: epithelial wing cells (cells/mm²), C: basal epithelial cells (cells/mm²), D: subbasal nerves ($\mu\text{m}/\text{mm}^2$), E: subepithelial keratocytes (cells/mm²).

* one-way repeated measures analysis of variance was used where normality and equal variance criteria were met. For normally-distributed data with unequal variance, a paired t-test was used, with p-values reported for the pairwise comparisons: Preoperative/4m, 4m/8m, and Preoperative/8m, respectively.

†Preoperative/4m significance was $P = 0.007$ and Preoperative/8m significance was $P = 0.055$ (Student-Newman-Keuls method).

‡§ values with the same symbol were significantly different

|| values differed significantly from each other ($p = 0.005$; independent t-test).

Statistically significant values ($p < 0.05$) are indicated **in bold**.